THE JOURNAL OF BIOLOGICAL CHEMISTRY VOL. 284, NO. 52, pp. 36357–36366, December 25, 2009
Printed in the U.S.A.

Identification of the Penta-EF-hand Protein ALG-2 as a Ca^{2+}-dependent Interactor of Mucolipin-1*[S]

Received for publication, July 21, 2009, and in revised form, October 21, 2009 Published, JBC Papers in Press, October 28, 2009, DOI 10.1074/jbc.M109.047241

Silvia Vergarajauregui, Jose A. Martina, and Rosa Puertollano[1]

From the Laboratory of Cell Biology, NHLBI, National Institutes of Health, Bethesda, Maryland 20892

Loss of function mutations in mucolipin-1 (MCOLN1) have been linked to mucolipidosis type IV (MLIV), a recessive lysosomal storage disease characterized by severe neurological and ophthalmological abnormalities. MCOLN1 is an ion channel that regulates membrane transport along the endolysosomal pathway. It has been suggested that MCOLN1 participates in several Ca^{2+}-dependent processes, including fusion of lysosomes with the plasma membrane, fusion of late endosomes and autophagosomes with lysosomes, and lysosomal biogenesis. Here, we searched for proteins that interact with MCOLN1 in a Ca^{2+}-dependent manner. We found that the penta-EF-hand protein ALG-2 binds to the NH-terminal cytosolic tail of MCOLN1. The interaction is direct, strictly dependent on Ca^{2+}, and mediated by a patch of charged and hydrophobic residues located between MCOLN1 residues 37 and 49. We further show that MCOLN1 and ALG-2 co-localize to enlarged endosomes induced by overexpression of an ATPase-defective dominant-negative form of Vps4B ($Vps4B^{E235Q}$). In agreement with the proposed role of MCOLN1 in the regulation of fusion/fission events, we found that overexpression of MCOLN1 caused accumulation of enlarged, aberrant endosomes that contain both early and late endosome markers. Interestingly, aggregation of abnormal endosomes was greatly reduced when the ALG-2-binding domain in MCOLN1 was mutated, suggesting that ALG-2 regulates MCOLN1 function. Overall, our data provide new insight into the molecular mechanisms that regulate MCOLN1 activity. We propose that ALG-2 acts as a Ca^{2+} sensor that modulates the function of MCOLN1 along the late endosomal-lysosomal pathway.

Mucolipidosis type IV (MLIV)[2] is an autosomal recessive disorder characterized by severe neurological and ophthalmological abnormalities. Symptoms appear during the 1st year of life and include mental retardation, delayed motor milestones, achlorhydria, and visual problems such us corneal clouding, retinal degeneration, sensitivity to light, and strabismus (1–3). Analysis of various cell types from MLIV patients by electron microscopy revealed the presence of enlarged vacuolar structures. These structures were found to accumulate a variety of lipids (phospholipids, gangliosides, and neutral lipids) and mucopolysaccharides forming multiconcentric lamellae, as well as granulated water-soluble materials (4–7). Unlike other lysosomal storage diseases, this accumulation is not attributable to defects in the catabolism of lipids and proteins but to a defective transport of membrane components along the late endosomal-lysosomal pathway (8, 9).

Loss-of-function mutations in the transmembrane protein mucolipin-1 (MCOLN1), also referred to as TRPML1, are the cause of MLIV (10–13). MCOLN1 is an ion channel that, together with MCOLN2 and MCOLN3, constitutes the TRPML subfamily within the transient receptor potential superfamily of ion channels (14). MCOLN1 is a 580-amino acid protein with a predicted topology of six transmembrane-spanning domains with both amino- and carboxyl-terminal tails having a cytosolic orientation and the pore located between transmembrane segments 5 and 6. Consistent with the lysosomal defects observed in MLIV, MCOLN1 localizes to late endosomes-lysosomes via two acidic di-leucine motifs individually located near the ends of the amino- and carboxyl-terminal tails (15, 16). Post-translational modifications play an important role in the regulation of MCOLN1 function. Palmitoylation and phosphorylation at the carboxyl-terminal tail modulate trafficking and channel activity, respectively (16, 17), although cleavage at the first luminal loop inactivates the protein (18). The selectivity of the MCOLN1 channel remains controversial, as different studies have suggested that the channel is permeable to Ca^{2+} (19), K^+, Ca^{2+}, and Na^+ (20), H^+ (21), and Fe^{2+} (22).

The accumulation of enlarged vacuolar structures observed in MLIV patients led to the suggestion that MCOLN1 may be involved in the regulation of the biogenesis of lysosomes, specifically in the reformation of lysosomes from endosome-lysosome hybrid organelles (23). This idea was supported by the observation that loss of the *Caenorhabditis elegans* orthologue of MCOLN1, *cup-5*, resulted in formation of enlarged hybrid organelles that contained both late endosomal and lysosomal markers (24). MCOLN1 has also been associated with lysosomal secretion, as fusion of lysosomes with the plasma membrane in response to Ca^{2+} was found to be impaired in MLIV cells (25). Recently, we have proposed that MCOLN1 may play a role in the fusion of both autophagosomes and late endosomes with lysosomes (26). Absence of MCOLN1 results in accumulation of autophagosomes and dysfunctional autophagy in

* This work was supported, in whole or in part, by a National Institutes of Health grant from NHLBI Intramural Research.

[S] The on-line version of this article (available at http://www.jbc.org) contains supplemental Figs. 1 and 2.

[1] To whom correspondence should be addressed: Laboratory of Cell Biology, NHLBI, National Institutes of Health, 9000 Rockville Pike, Bldg. 50/3537, Bethesda, MD 20892. Tel.: 301-451-2361; Fax: 301-402-1519; E-mail: puertolr@mail.nih.gov.

[2] The abbreviations used are: MLIV, mucolipidosis IV; MCOLN1, mucolipin-1; GFP, green fluorescent protein; GST, glutathione *S*-transferase; PRR, proline-rich region; ABH, acidic-basic-hydrophobic; ABS, ALG-2 binding sequence; PBS, phosphate-buffered saline; ER, endoplasmic reticulum.

MLIV cells (26–28). Additional roles for MCOLN1 have been suggested, including regulation of lysosomal acidification (21, 29), chaperone-mediated autophagy (30), and Fe^{2+} release from late endosomes and lysosomes (22).

Notably, most of the cellular processes thought to be regulated by MCOLN1 (*i.e.* fusion of late endosomes and lysosomes, biogenesis of lysosomes, lysosomal exocytosis, and autophagy) are processes that require Ca^{2+} (31–33). The permeability of the MCOLN1 channel is still not well understood. However, most of the studies regarding this subject propose that MCOLN1 is a Ca^{2+}-permeable channel, and the activity is regulated by changes in Ca^{2+} concentration on either the cytosolic or luminal face of the membrane, thus indicating that Ca^{2+} is an important modulator of MCOLN1 function (20, 34). Furthermore, when a proline substitution was introduced into MCOLN1 to resemble the form of MCOLN3 known to cause the varitint-waddler (Va) mouse phenotype (TRPML1*V432P*), the resulting channel activity was inwardly rectifying, Ca^{2+}-selective, proton-impermeable, and activated by low pH, further supporting a role for MCOLN1 as a Ca^{2+} channel that drives membrane fusion events within the endosomal pathway (35, 36).

To better understand the mechanisms that regulate MCOLN1 function, we decided to search for proteins that interact with MCOLN1 in a Ca^{2+}-dependent manner. In this study, we report a Ca^{2+}-dependent interaction between MCOLN1 and ALG-2 (apoptosis-linked gene-2). ALG-2 is a Ca^{2+}-binding protein that belongs to the penta-EF-hand protein family (37). ALG-2 functions as a Ca^{2+}-sensor by changing its conformation and hence affinities to its binding partners in a Ca^{2+}-dependent manner (37–39). Based on the interaction of ALG-2 with Alix/AIP (40, 41), TSG101 (42), and Sec31A (43–45), ALG-2 has been suggested to regulate membrane trafficking at both the endosomal and ER-Golgi pathways. In addition, ALG-2 has been implicated in neuronal death during development (46), regulation of ER-stress-induced apoptosis (47), and cancer (48). Here, we show that ALG-2 binds to the amino-terminal tail of MCOLN1 in a Ca^{2+}-dependent manner. We identified the residues in MCOLN1 responsible for this interaction and demonstrated that both proteins co-localize to endosomes. Mutation of the ALG-2-binding domain in MCOLN-1 led to defects in its distribution and function, suggesting that ALG-2 regulates MCOLN1 activity. Altogether, our data give new insight on the molecular basis for the regulation of MCOLN1 function by Ca^{2+}.

EXPERIMENTAL PROCEDURES

Antibodies and Reagents—The following antibodies were used: rabbit anti-GFP (MBL International, Woburn, MA), rabbit anti-ALG-2 (Swant, Bellinzona, Switzerland), mouse anti-Sec31A (BD Biosciences), rabbit anti-Hrs (Novuls Biologicals, Littleton, CO), mouse anti-CD63 (clone H5C6; Pharmingen), mouse anti-FLAGM2 (Sigma), mouse anti-His (Novagen, Madison, WI), and mouse anti-actin (Sigma). FuGENE 6 reagent and protease inhibitor mixture tablets were obtained from Roche Applied Science.

Plasmids—GST-MCOLN1-NTail and GST-MCOLN1-CTail were cloned as described previously (17). To generate the truncated forms of GST-MCOLN1-NTail, we introduced either an EcoRI site in the corresponding 5′ site of the truncated construct and recloned it into the EcoRI and SalI sites of pGEX51 vector or introduced a stop codon at the corresponding amino acid. To generate GFP-MCOLN1, full-length MCOLN1 was cloned into the EcoRI and SalI sites of the pEGFPC2 vector (Clontech). Construction of MCOLN1-FLAG was described previously (17). Mutations of residues in the cytosolic tail of MCOLN1 were introduced using the QuickChange site-directed mutagenesis kit, as per the manufacturer's instructions (Stratagene, La Jolla, CA). The complete open reading frame of human ALG-2 was PCR-amplified from a placenta cDNA library using specific primers and cloned into the EcoRI and SalI sites of pEGFP-C2 and the Cherry-C2 vectors (Clontech) and His-Parallel vector. The point mutations at the first and third EF-hands of ALG-2 were introduced by QuickChange site-directed mutagenesis kit to generate pEGFP-C2-ALG2$^{E47A/E114A}$. The alternatively spliced isoform of ALG-2 was constructed by deleting amino acids GF^{122} using the QuickChange site-directed mutagenesis kit. Site-directed mutations were confirmed by subsequent DNA sequencing. GFP-hVps4B^{E235Q} was a kind gift of P. Woodman (University of Manchester, Manchester, UK).

Cell Culture, Transfection, and siRNA Knockdown—HeLa and HEK293 cells were maintained in Dulbecco's modified Eagle's medium (Invitrogen) supplemented with antibiotics and 10% fetal bovine serum. The human retinal pigmented epithelial cell line ARPE19 was grown in a 1:1 mixture of Dulbecco's modified Eagle's medium and Ham's F-12 media supplemented as above. Cells were transiently transfected using FuGENE 6 (Roche Applied Science) according to the manufacturer's recommendations. Transfected cells were analyzed 24 h post-transfection. For ALG-2 knockdown, cells were transfected with either siRNA against ALG-2 or nontargeting siRNA using DharmaFect transfection reagent (Dharmacon-ThermoScientific, Lafayette, CO). Treated cells were lysed 72 h after transfection.

GST Pulldown—GST fusion proteins were expressed in bacteria and affinity-purified by standard methods. HeLa cells were washed with ice-cold PBS and lysed in buffer B (25 mM Hepes, 250 mM NaCl, 1% Triton X-100, and 1 mM dithiothreitol, pH 7.4) supplemented with 1 mM $CaCl_2$ and protease inhibitors. The lysate was precleared by centrifugation and incubated with 100 μg of GST fusion protein immobilized on glutathione beads for 3 h at 4 °C. Beads were washed four times with buffer B and transferred to a column. Bound proteins were eluted with 10 mM EGTA, separated by SDS-PAGE (4–20% gradient gels) under reducing conditions, visualized by Coomassie Blue staining, and excised from the gel.

Mass Spectrometry and Protein Identification—Excised bands were destained using 25 mM NH_4HCO_3, 50% acetonitrile for 10-min intervals until completely destained. Gel samples were then dried, reduced with 10 mM dithiothreitol in 25 mM NH_4HCO_3 for 1 h at 56 °C, and alkylated with 55 mM iodoacetamide in 25 mM NH_4HCO_3 for 45 min at room temperature in darkness. Upon supernatant removal, gels were washed with 25 mM NH_4HCO_3 for 10 min and with 25 mM NH_4HCO_3/50% acetonitrile and then dried. Proteins in gels were trypsinized

using 12.5 ng/μl sequencing-grade modified trypsin (Promega, Madison, WI) diluted in 25 mM NH_4HCO_3 and incubated at 37 °C for 16 h. Peptides were collected from digest solutions, lyophilized to near dryness, and reconstituted with 15 μl of 0.1% formic acid.

Liquid chromatography-tandem mass spectrometry analyses were carried out using an Agilent 1100 nanoflow LC system (Palo Alto, CA) connected to a Finnigan LTQ mass spectrometer (Thermo Scientific, San Jose, CA), as described previously (49). Briefly, peptides were first loaded onto a peptide trap cartridge (Agilent, Palo Alto, CA) at a flow rate of 2 μl/min. Trapped peptides were then eluted onto a reversed-phase PicoFrit column (New Objective, Woburn, MA) and separated using a linear gradient of acetonitrile (0–60%) in 0.1% formic acid. The gradient time was 45 min at a flow rate of 0.25 μl/min. Eluted peptides from the PicoFrit column were sprayed into the LTQ mass spectrometer equipped with a nano-spray ion source. Data-dependent acquisition mode was enabled, and each survey MS scan was followed by five MS/MS scans with the dynamic exclusion option on. The spray voltage was 2 kV, and the temperature of ion transfer tube was set at 160 °C. The normalized collision energy was set at 35%.

Data base search for protein identification was carried out on an 8-node computer cluster using the SEQUEST search algorithm in BioWorks 3.3 (Thermo Scientific, San Jose, CA). Human RefSeq protein sequences (target) were downloaded from the NCBI website, and a reversed version of these sequences (decoy) was appended to the target sequence data base before performing data base searches. Only the best peptide match from each MS/MS spectrum was retained for further analysis. Phospho-PIC, an in-house computer program (50), was applied for automated filtering of peptide identifications by XCorr scores to achieve a false discovery rate of about 5% based on the number of decoy matches.

In Vitro Binding Assays—GST or GST fusion proteins (0.1 mg/ml) were incubated with recombinant His-ALG-2 in 0.5 ml of 50 mM Hepes-KOH, pH 7.5, 150 mM NaCl, 1 mM $MgCl_2$, 10% (v/v) glycerol, and 0.6 mg/ml bovine serum albumin in the presence of 1 mM $CaCl_2$ for 30 min at room temperature. Glutathione-Sepharose 4B (50 μl) was added and the incubation continued for an additional 30 min. The suspension was transferred to chromatography columns, washed extensively, and fist eluted in 10 mM EGTA and then in 20 mM glutathione. Samples were analyzed by SDS-PAGE and immunoblotting with antibody to the His tag.

Electrophoresis and Immunoblotting—Cells were washed with ice-cold PBS and lysed in buffer B (25 mM Hepes, 250 mM NaCl, 1% Triton X-100, and 1 mM dithiothreitol, pH 7.4) supplemented with protease inhibitors and subjected to pulldown analysis. Bound proteins were analyzed by SDS-PAGE (4–20% gradient gels) under reducing conditions and transferred to nitrocellulose. The nitrocellulose membrane was then blocked with PBS, 0.05% Tween 20, 10% nonfat milk and incubated with the indicated antibodies. Enhanced chemiluminescence reagent (Amersham Biosciences) was used for detection.

Immunofluorescence Microscopy—For immunofluorescence, cells were grown on glass coverslips and fixed in methanol/acetone (1:1, v/v) for 10 min at −20 °C. Incubation with primary antibodies diluted in PBS, 0.1% (w/v) saponin, and 0.1% bovine serum albumin was carried out for 1 h at room temperature. Unbound antibodies were removed by rinsing with PBS for 5 min, and cells were subsequently incubated with a secondary antibody (Alexa555- or Alexa488-conjugated goat anti-rabbit or anti-mouse Ig) diluted in PBS, 0.1% (w/v) saponin, and 0.1% bovine serum albumin for 30–60 min at room temperature. After a final rinse with PBS, coverslips were mounted onto glass slides with Fluoromount G (Southern Biotechnology Associates, Birmingham, AL). Fluorescence images were acquired on an LSM 510 confocal microscope (Carl Zeiss, Thornwood, NY). For co-localization analysis, the percentage of co-localized vesicles was calculated as the number of GFP-MCOLN1-positive vesicles that co-localized with the indicated organelle marker divided by the total number of GFP-MCOLN1-positive vesicles in a given cell and multiplied by 100.

RESULTS

Identification of Ca^{2+}-dependent Interactors of MCOLN1—Recent evidence has suggested the participation of MCOLN1 in several Ca^{2+}-dependent processes, including lysosomal exocytosis and fusion of autophagosomes and late endosomes with lysosomes. To better understand the mechanism of MCOLN1 function, we searched for proteins that interact with MCOLN1 in a Ca^{2+}-dependent manner. The soluble proteins representing the amino-terminal tail (GST-MCOLN1-NTail; residues 1–66) and the carboxyl-terminal tail (GST-MCOLN1-CTail; residues 518–580) of MCOLN1 were synthesized in bacteria as GST fusion proteins (Fig. 1*A*). Following purification, these fusion proteins were incubated with HeLa lysates in the presence of 1 mM $CaCl_2$. GST alone was used as a negative control. After extensively washing, proteins bound to MCOLN1 in a Ca^{2+}-dependent manner were eluted by adding the Ca^{2+} chelator EGTA, separated by SDS-PAGE, and visualized by Coomassie staining. Although no noticeable bands were observed in the GST or GST-MCOLN1-CTail pulldowns, three apparent bands were eluted when using the GST-MCOLN1-NTail (Fig. 1*B*). The three bands were excised from the gel, trypsinized, and subjected to mass spectrometry analysis. Bands B1 and B2 were identified as the members of the COPII complex Sec31A and Sec13, respectively, and band B3 was identified as the penta-EF-hand protein ALG-2.

To verify our mass spectrometry results, we performed Western blot analysis using specific antibodies. As expected, antibodies against Sec31A and ALG-2 detected the presence of these proteins in the eluted fractions of the GST-MCOLN1-NTail pulldowns. In contrast, no Sec31A or ALG-2 was observed in the GST-MCOLN1-CTail and GST pulldowns (Fig. 1*C*). The lack of a commercially available antibody against Sec13 prevented us from verifying the identity of B2 by immunoblot; however, the fact that Sec13 and Sec31A form a stable complex (51) suggests that the band B2 does indeed correspond to Sec13.

MCOLN1 Interacts with the Penta-EF-hand Protein ALG-2—An interaction between ALG-2 and Sec31A has been described previously (43, 45). ALG-2 binds very strongly to Sec31A at the endoplasmic reticulum exit sites, stabilizing the localization of Sec31A at these sites. ALG-2 also interacts with several endo-

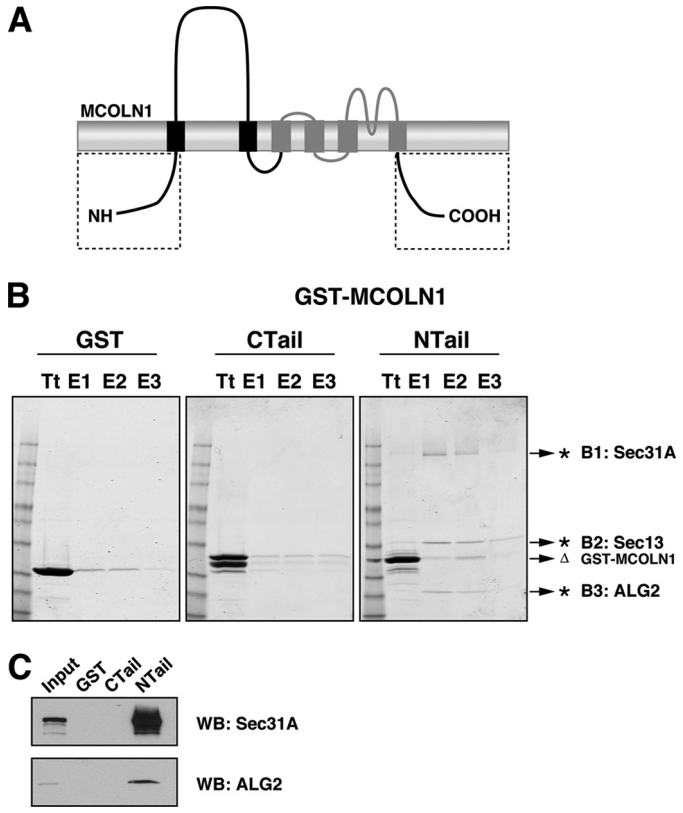

FIGURE 1. **Search for Ca^{2+}-dependent interactors of MCOLN-1.** *A,* proposed topology of MCOLN1 is shown, with the transient receptor potential (*TRP*) domain depicted in *gray*, and the two cytosolic tails denoted by *squares*. *B,* HeLa cells were lysed, and the cleared lysate was incubated with glutathione-Sepharose beads carrying GST, GST-MCOLN1-Ctail, or GST-MCOLN1-NTail in the presence of 1 mM $CaCl_2$. After washing, bound proteins were eluted with 10 mM EGTA and collected in three elutions (E1, E2, and E3). A small fraction of the pulldown was recovered before eluting (*Tt*). Total pulldowns and protein eluates were separated on denaturing SDS-polyacrylamide gels and visualized by Coomassie staining. Bands B1, B2 and B3, indicated by *asterisks*, were excised from the gel, digested with trypsin, and subjected to mass spectrometry analysis. The band representing GST-MCOLN1 is indicated by Δ. Excluding keratins, the number of peptide hits for a protein relative to the number of total peptide hits in a band was 225 out of 241 for Sec31A (B1), 47 out of 56 for Sec13 (B2), and 70 out of 72 for ALG-2 (B3). *C,* identity of Sec31A and ALG-2 was corroborated by immunoblotting using specific antibodies. *WB*, Western blot.

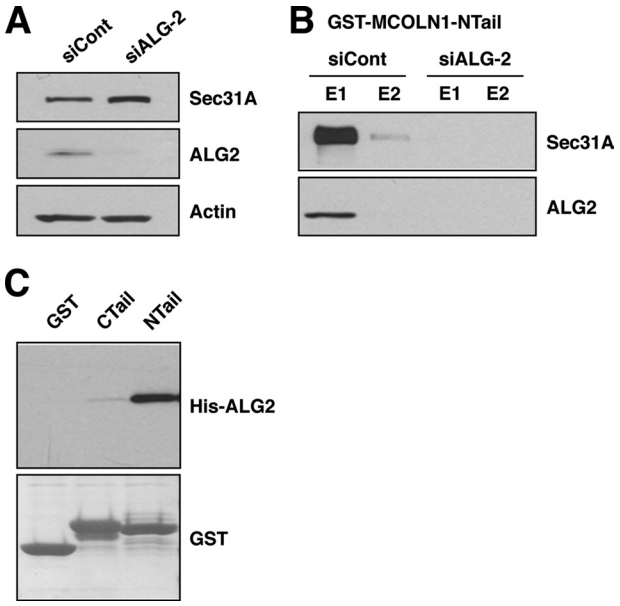

FIGURE 2. **Depletion of ALG-2 eliminates Sec31A from the elution fractions.** *A,* HeLa cells were transfected with nontarget small interfering RNA (*siCont*) or siRNA targeted to ALG-2 (*siALG-2*). Seventy two hours after transfection, cells were lysed, and equivalent amounts of homogenate were subjected to SDS-PAGE and immunoblotted with antibodies to Sec31A, ALG-2, and actin (loading control). *B,* lysates from siControl and siALG-2 were incubated with GST-MCOLN1-NTail in the presence of 1 mM $CaCl_2$. After washing, bound proteins were eluted with 10 mM EGTA (*E1* and *E2*), separated on denaturing SDS-polyacrylamide gels, and analyzed by Western blotting. *C,* recombinant His-ALG-2 (50 μg/ml) was tested for interactions with GST or GST fusion proteins bearing the C- and N-tails of MCOLN1 in the presence of Ca^{2+}. Bound His-ALG2 was eluted with 10 mM EGTA, and GST fusion proteins were eluted with 20 mM glutathione. The GST fusion proteins were visualized by Ponceau staining, and bound His-ALG-2 was detected by immunoblotting with antibody to His.

somal proteins such as Alix/AIP1 (40, 41), TSG101 (42), and the annexins VII/XI (52, 53), suggesting a role for ALG-2 in the regulation of trafficking along the endosomal pathway. In addition, ALG-2 has been shown to be present at Lamp-1-enriched fractions after subcellular fractionation, further indicating an association of ALG-2 with late endosomes/lysosomes (42). Given the primary location of MCOLN1 to late endosomes/lysosomes (16) and the fact that ALG-2 is the only Ca^{2+}-binding protein identified in the eluted fractions, we reasoned that MCOLN1 interacts with ALG-2, although the presence of Sec31A and Sec13 at the GST-MCOLN1-NTail pulldowns is indirect and due to the ability of Sec31A to bind ALG-2.

To test this hypothesis, we depleted endogenous ALG-2 in HeLa cells by using specific small interfering RNAs (siALG-2). As shown in Fig. 2*A*, the levels of ALG-2 were reduced 95% in siALG-2-treated cells when compared with cells treated with a control nontarget siRNA (siControl). In contrast, the levels of Sec31A were not affected by treatment with siALG-2 or siControl (Fig. 2*A*). Next, we performed pulldown experiments by incubating GST-MCOLN1-NTail with cell extracts from siALG-2- or siControl-treated cells. As predicted, we found that Sec31 was not pulled down by GST-MCOLN1-NTail in the absence of ALG-2 (Fig. 2*B*). Analysis of the eluted fractions by silver staining revealed that the band corresponding to Sec13 was lost in siALG-2-treated cells as well (data not shown). Therefore, our results indicate that MCOLN1 does not interact directly with the Sec31A-Sec13 complex and that the presence of COPII subunits in the GST-MCOLN1-NTail pulldowns might be due to the ability of Sec31A to bind ALG-2.

To confirm direct binding between ALG-2 and MCOLN1, we carried out pulldown experiments using recombinant His-ALG2 in the presence of Ca^{2+}. As seen in Fig. 2*C*, ALG-2 bound GST-MCOLN1-NTail, although GST alone or GST-MCOLN1-CTail did not produce any detectable signal, thus corroborating that ALG-2 directly interacts with the NH-terminal cytosolic tail of MCOLN1.

Interaction between ALG-2 and MCOLN1 Is Dependent on Ca^{2+}—The interaction between MCOLN1 and ALG-2 was found in pulldown experiments performed in the presence of 1 mM Ca^{2+}. To check whether the two proteins can interact under more physiological conditions, we performed pulldown assays in the presence of a wider range of Ca^{2+} concentration or in the presence of the Ca^{2+} chelator EGTA. As seen in Fig. 3*A*, the amount of endogenous ALG-2 pulled down by MCOLN1-

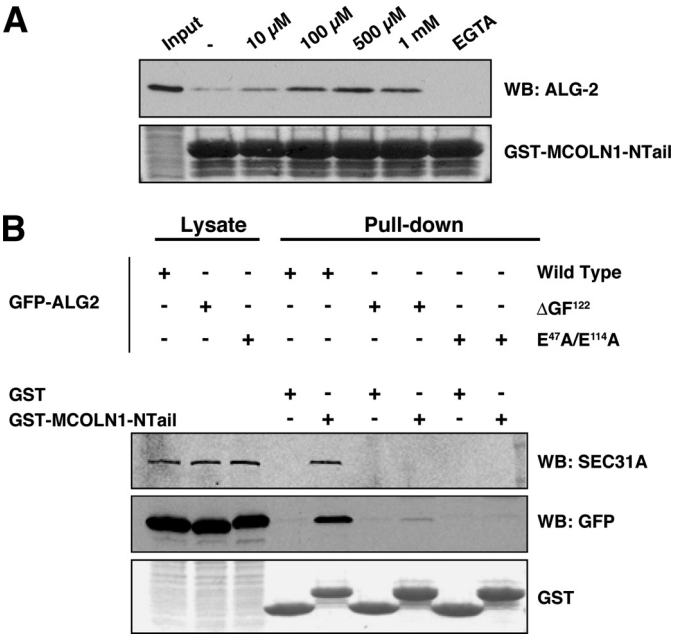

FIGURE 3. **Ca^{2+}-dependent binding of ALG-2 to GST-MCOLN1-NTail.** *A*, HeLa cells were lysed, and the cleared lysate was incubated with glutathione-Sepharose beads carrying GST-MCOLN1-NTail in the absence (−) or presence of increasing concentrations of $CaCl_2$ or in the presence of 10 mM EGTA. After washing, the pulldown products were analyzed by Western blotting (*WB*) using an anti-ALG2 antibody. Ponceau staining showed similar levels of fusion protein in each well. *B*, cleared lysates of HEK293 cells expressing GFP-ALG-2 (wild type), GFP-ALG-2Δ^{GF122} (ΔGF^{122}), or GFP-ALG-$2^{E47A/E114}$ (*E47A/E114A*) were subjected to GST or GST-MCOLN1-NTail pulldown assays in the presence of 1 mM $CaCl_2$, and the pulldown products were analyzed by Western blotting using either anti-GFP or anti-Sec31A antibodies.

NTail was barely detectable when the experiments were performed in the absence of Ca^{2+}. Increasing Ca^{2+} concentration led to a more efficient interaction between MCOLN1 and ALG-2, reaching a peak at 0.5 mM $CaCl_2$. In contrast, no interaction was detected in the presence of EGTA (Fig. 3*A*).

To further confirm the Ca^{2+} dependence for the interaction of MCOLN1 and ALG-2, we tested the ability of MCOLN1 to bind to a Ca^{2+}-binding defective ALG-2 mutant, in which the two glutamic acid residues located in the high affinity Ca^{2+}-binding motifs EF1 and EF3 were mutated to Ala (ALG-$2^{E47A/E114A}$) (37). GFP-ALG-2 and GFP-ALG-$2^{E47A/E114A}$ were expressed in HEK293 cells, and their binding capacity to MCOLN1 was measured by pulldown assays in the presence of Ca^{2+}. Although GFP-ALG-2 wild type was efficiently pulled down by GST-MCOLN1-NTail, the GFP-ALG-$2^{E47A/E114A}$ mutant failed to interact with MCOLN1 (Fig. 3*B*), thus indicating that ALG-2 needs to bind Ca^{2+} to bind MCOLN1.

We also tested the binding capacity of an alternatively spliced isoform of ALG-2, which lacks two amino acids (ΔGF^{122}) and has a lower affinity for Ca^{2+} than full-length ALG-2 (54). As expected, the ability of the ΔGF^{122} isoform to bind MCOLN1 was drastically reduced when compared with ALG-2 full-length (Fig. 3*B*). These data indicate that MCOLN1 belongs to the isoform noninteractive group of ALG-2 interactors, which also include Alix and TSG10 (55). It is important to note that Sec31A was not present in the pulldowns performed with GFP-ALG-$2^{E47A/E114A}$ or ΔGF^{122}, thus confirming that there is not a direct interaction between MCOLN1 and Sec31A (Fig. 3*B*).

Identification of the ALG-2 Binding Domain in MCOLN1—Next, we investigated the MCOLN1 domain responsible for the interaction with ALG-2. ALG-2 is known to interact with proteins containing proline-rich regions (PRR) (42). A region containing the P*X*Y repeats was shown to be sufficient for binding of ALG-2 to Alix/AIP1 (56, 57). Looking at the primary sequence of MCOLN1, we identified several proline residues and one P*X*Y motif that seem to be highly conserved through evolution (Fig. 4*A*). To test whether this proline-rich region in MCOLN1 was necessary for the interaction with ALG-2, we generated truncated mutants of the NH-tail of MCOLN1 fused to GST and performed GST pulldown assays with HeLa extracts in the presence of 1 mM $CaCl_2$. As seen in Fig. 4, *A* and *B*, deletion of the MCOLN1 PRR did not abrogate interaction with ALG-2, as the MCOLN1-NTail-(37–66) mutant still retained the ability to pulldown ALG-2. Mutation of Pro^{18-20} and Pro^{28-30} to alanines did not affect the interaction either (data not shown). Moreover, a chimera that just contains the MCOLN1 PRR (MCOLN1-NTail-(1–37)) was unable to bind ALG-2, indicating that MCOLN1 belongs to the group of proteins that do not require a PRR to interact with ALG-2 (58, 59).

In contrast, those chimeras that include a region enriched in charged and hydrophobic amino acids (ABH) (residues from position 37 to 49) (MCOLN1-NTail-(1–66), MCOLN1-NTail-(25–66), MCOLN1-NTail-(37–66), and MCOLN1-NTail-(1–49)) retained the capability to pull down ALG-2, although truncation of this region (MCOLN1-NTail-(1–41) and MCOLN1-NTail-(42–66)) abolished the binding (Fig. 4, *A* and *B*). To further identify the residues responsible for the interaction between MCOLN1 and ALG-2, we performed alanine scanning mutagenesis of the ALG-2-binding domain of MCOLN1. Substitution of the acidic residues E39D or the hydrophobic residues ^{47}YFF to alanine reduced the interaction with ALG-2, although substitution of residues ^{44}RLK to alanine abrogated the binding entirely (Fig. 4*C* and supplemental Fig. 1). Moreover, introduction of individual mutations within the RLK triplet revealed that substitution of either Arg^{44} or Leu^{45} by alanine strongly decreased the affinity for ALG-2, although mutation of Lys^{46} alone did not affect the binding (Fig. 4*D*). Once again, Sec31A was not pulled down by the MCOLN1 mutants that failed to bind ALG-2 (Fig. 4 and supplemental Fig. 1). Altogether our data indicate that a patch of acidic-basic and hydrophobic residues in the NH-tail of MCOLN1 is responsible for the interaction with ALG-2 and that the amino acids Arg^{44} and Leu^{45} play a critical role in the binding.

MCOLN1 and ALG-2 Co-localize to Vps4B^{E235Q}-induced Enlarged Endosomes—As mentioned previously, the ability of ALG-2 to bind several endosomal proteins suggests a role of ALG-2 in endosomal function; however, the association of ALG-2 with endosomal membranes is transient. Proteins that localize transiently in endosomes are known to accumulate in aberrant endosomal compartments in cells expressing the dominant-negative AAA ATPase Vps4B (Vps4B^{E235Q}) (60, 61). Moreover, Katoh *et al.* (42) described that in HeLa cells transiently expressing GFP-tagged Vps4B^{E235Q}, ALG-2 was recruited to perinuclear structures that colocalize with GFP-Vps4B^{E235Q} in a Ca^{2+}-dependent manner. To determine whether ALG-2 and MCOLN1 co-localize into the same subcellular compartment, we

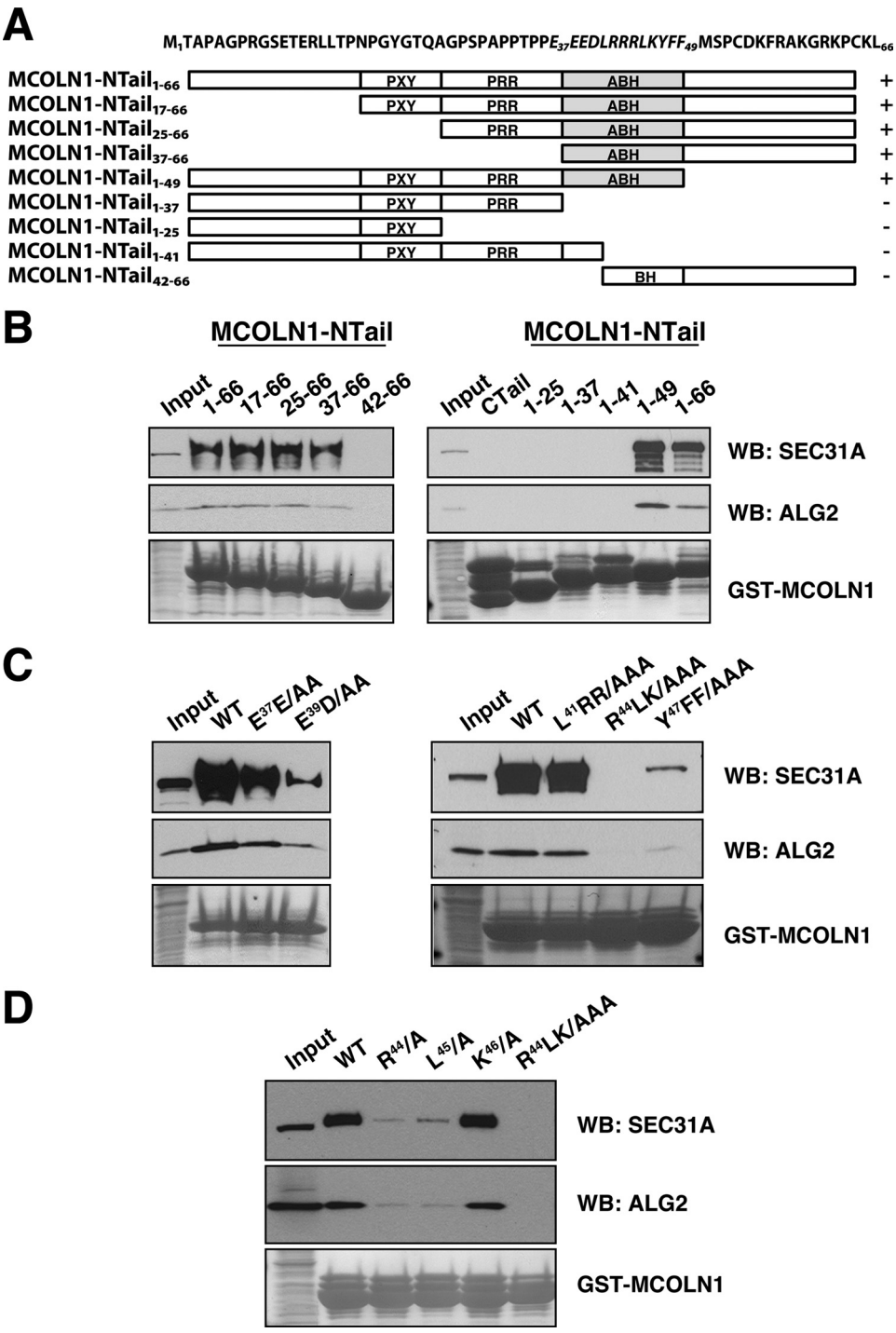

FIGURE 4. **Identification of the ALG-2 binding domain in MCOLN1.** *A,* schematic representation of the different motifs found in MCOLN1-NTail as well as the truncated forms used in the pulldown assays. The binding capacity of the chimeras to ALG-2 is indicated on the *right*. The domain identified as required for ALG-2 binding is shown in *italics* and corresponds to the ABH domain. *B,* truncated forms of GST-MCOLN1-NTail shown in *A* were generated and subjected to pulldown experiments using HeLa precleared lysates in the presence of 1 mM $CaCl_2$. *C* and *D,* individual mutations were introduced into the MCOLN1-NTail ABH domain, and the corresponding GST recombinant proteins were subjected to pulldown analysis. Pulldown products were analyzed by Western blotting (*WB*) using anti-ALG-2 and anti-Sec31A antibodies.

transiently expressed GFP-Vps4B^{E235Q}, Cherry-ALG-2, and MCOLN1-FLAG in the human retinal pigmented epithelial cell line ARPE19 (62, 63) and analyzed the localization of the three proteins by confocal microscopy. As seen in Fig. 5, expression of GFP-Vps4B^{E235Q} leads to the recruitment of Cherry-ALG-2 into GFP-positive endosomes as reported previously (42). Immunofluorescence analysis with an antibody against FLAG revealed that MCOLN1 was also present in Vps4B^{E235Q}/ALG-2 positive endosomes (Fig. 5, *insets*) indicating that MCOLN1 and ALG-2 co-localize to endosomes.

ALG-2 Regulates the Activity of MCOLN1 in the Endosomal Pathway—To understand the physiological role of the interaction between ALG-2 and MCOLN1, we sought to study the distribution and function of an ALG-2-binding defective mutant of MCOLN1. To do so, we substituted the ^{44}RLK residues to alanine in the MCOLN1 full-length protein (GFP-MCOLN1-RLK) and addressed the distribution of mutant *versus* wild type MCOLN1 (GFP-MCOLN1-wt) transiently expressed in ARPE19 cells. We have previously described that MCOLN1 co-localizes with the late endosomal/lysosomal marker CD63 in HeLa cells. Moreover, overexpression of MCOLN1 causes swelling of CD63-positive structures resembling the accumulation of enlarged vacuoles observed in cells from MLIV patients (16). Expression of GFP-MCOLN1-wt in ARPE19 cells also caused aggregation of enlarged late endosomes/lysosomes at the perinuclear area (Fig. 6, *A* and *C*). In contrast, the GFP-MCOLN1-RLK mutant showed a decreased co-localization with CD63 (61.13% co-localization between MCOLN1-wt and CD63 *versus* 45.8% co-localization between MCOLN1-RLK and CD63) and was much less efficient promoting accumulation of enlarged CD63-labeled vesicles (Fig. 6, *A* and *D*). To ensure that the difference in subcellular localization was not due to different levels of expression of the two constructs, we analyzed the two fusion proteins by SDS-PAGE and immunoblotted with an antibody against GFP. As seen in Fig. 6*B*, both proteins were similarly expressed and were able to oligomerize (upper bands) and undergo proteolytic cleavage (lower band) (17, 18, 64).

Remarkably, many of the enlarged CD63-positive structures induced by expression of MCOLN1-wt also contained early

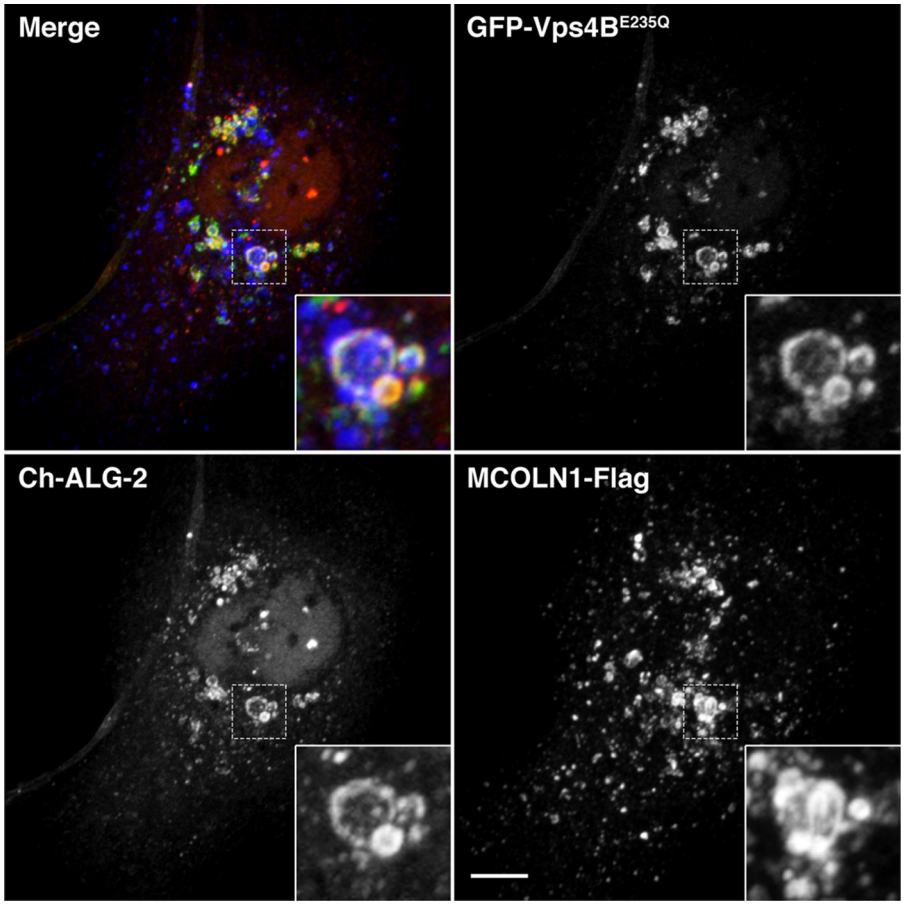

FIGURE 5. **ALG-2 and MCOLN1 co-localize to Vps4B^{E235Q}-induced enlarged endosomes.** ARPE19 cells were co-transfected with pEGFP-Vps4B^{E235Q}, Cherry-ALG-2, and MCOLN1-FLAG. After 24 h of transfection, cells were fixed and analyzed by confocal microscopy. Note that expression of the dominant-negative AAA ATPase Vps4 (Vps4^{E235Q}) causes the accumulation of Ch-ALG-2 on endosomal membranes where MCOLN1-FLAG is present. *Insets* are 3-fold magnifications of the indicated regions. GFP-Vps4 B^{E235Q} is in *green*, Cherry-ALG-2 is in *red*, and MCOLN1-FLAG is in *blue*. *Scale bar*, 10 μm.

endosomal proteins such as Hrs-1, whereas in nontransfected cells the co-localization between these two proteins was very limited (Fig. 6*C*). This indicates that MCOLN1-wt promotes the formation of aberrant endosomes that contain both early and late endosomes markers. Quantification of multiple random fields of cells revealed that 38.9% of the GFP-MCOLN1-wt structures also contained Hrs and CD63 (Fig. 6*D*). In contrast, endosomal aggregation was greatly reduced when the ALG-2 defective binding mutant GFP-MCOLN1-RLK was expressed in ARPE19 cells, with only 28% of the MCOLN1-RLK-positive vesicles containing both Hrs and CD63 (Fig. 6*D*). In addition, quantification of the distribution of CD63 by confocal microscopy revealed that MCOLN1-wt was significantly more efficient than MCOLN1-RLK promoting aggregation of CD63-positive vesicles at the perinuclear region. Thus, for example, 80% of CD63 vesicles were concentrated within a 10-μm radius from the center of the nucleus in MCOLN1-wt-expressing cells, whereas only 54% of CD63 structures were accumulated in the same area in cells expressing MCOLN1-RLK (supplemental Fig. 2). All together, our data indicate that binding of MCOLN1 to ALG-2 plays an important role in the regulation of the distribution and function of MCOLN1.

DISCUSSION

In this study, we report a novel Ca^{2+}-dependent interaction between MCOLN1 and the penta-EF-hand protein ALG-2. We found that ALG-2 directly binds to the amino-terminal cytosolic tail of MCOLN1, thus regulating MCOLN1 function at the endosomal/lysosomal pathway.

The interaction between ALG-2 and MCOLN1 is dependent on Ca^{2+} as revealed by the lack of binding in the presence of EGTA. In resting cells, the cytosolic Ca^{2+} concentration is usually less than 1 μM explaining the very weak ALG-2/MCOLN1 interaction observed in the absence of exogenously added Ca^{2+}. In contrast, free Ca^{2+} is highly concentrated in lysosomes (65). It has been reported that in macrophages the luminal Ca^{2+} concentration in lysosomes may be as high as 400–600 μM. This high Ca^{2+} concentration is maintained in part by the proton gradient across lysosomal membranes (65). Changes in lysosomal pH lead to increases in cytosolic Ca^{2+} indicating that lysosomes can provide an intracellular source for physiological increases in cytosolic Ca^{2+} levels (65). We propose that increases in Ca^{2+} levels in the vicinity of lysosomes may be high enough to promote efficient interaction between ALG-2 and MCOLN1.

In recent years, a growing number of ALG-2-binding proteins have been identified. Some of these proteins, such as Alix (40, 41), annexin VII (53), annexin XI (52, 53), and TSG101 (42) contain sequences rich in proline, glycine, and tyrosine, suggesting a consensus sequence PPYP(X_{3-5})YP (where *X* is an uncharged amino acid). In contrast, Sec31A (43–45) and Scotin (66) do not conform to the consensus sequence despite containing a segment rich in proline and tyrosine, whereas Ask-1 (59) and Raf-1 (58) do not possess any conspicuous proline-rich regions. The amino-terminal tail of MCOLN1 contains a region rich in proline residues that include a ^{20}P*X*Y motif and the sequence ^{28}PSPAPPTPP^{36}. However, a MCOLN1 mutant whose PRR domain was deleted retained its capacity to bind ALG-2, indicating that the PRR domain in MCOLN1 is not required for the interaction between MCOLN1 and ALG-2. Instead, we identified MCOLN1 amino acids 37–49 as a new ALG-2-binding domain. This domain consists of a stretch of charged (acidic and basic) and hydrophobic amino acids (^{37}EEEDLRRRLKYFF^{49}). Disruption of this domain abrogates the interaction between MCOLN1 and ALG-2 suggesting that the net electrostatic charge of the domain may be important for

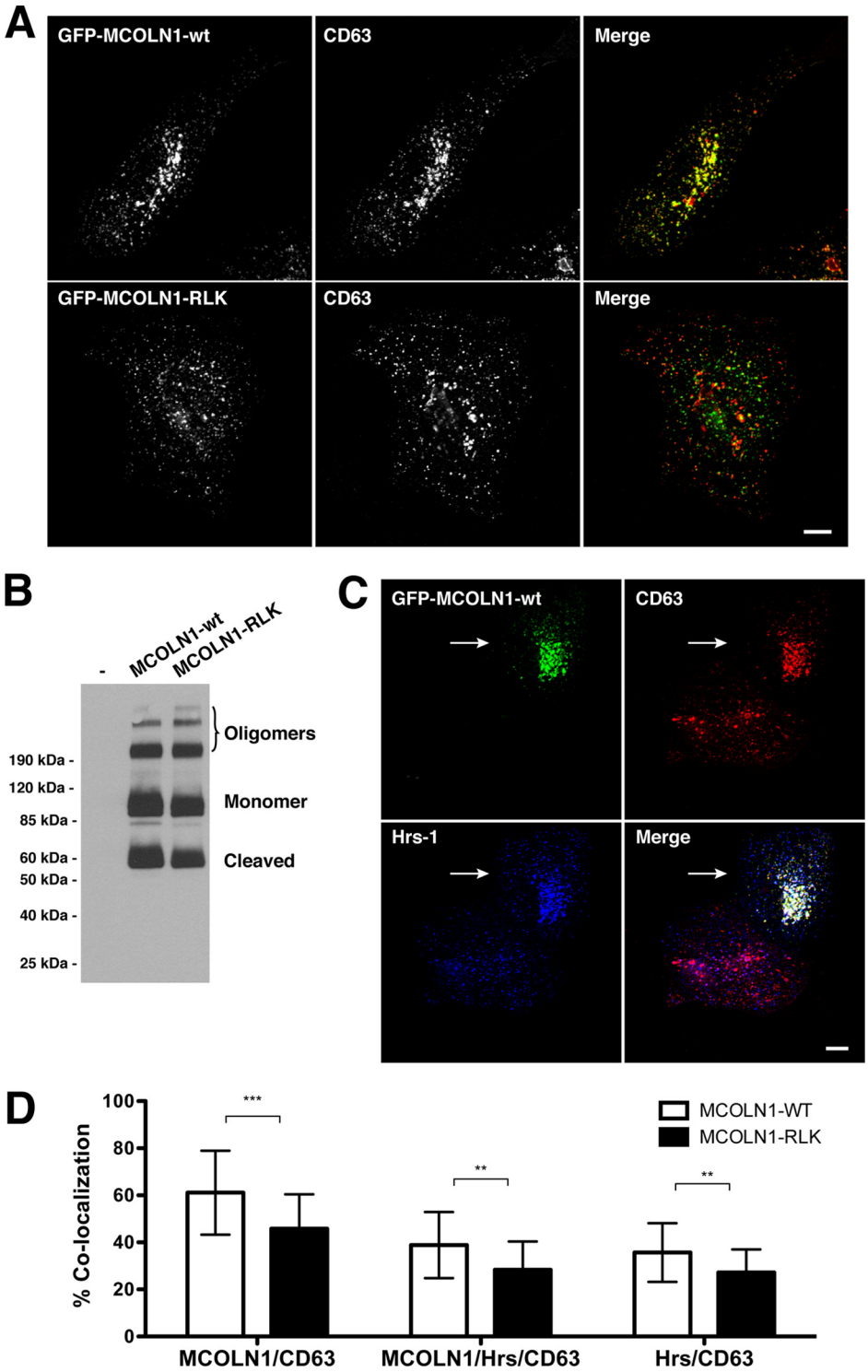

FIGURE 6. **ALG-2 regulates MCOLN1 activity at the endosomal pathway.** *A,* ARPE19 cells were transfected with GFP-MCOLN1-WT (*upper row*) or the ALG-2-binding defective mutant GFP-MCOLN1-^{44}RLK/AAA (RLK) (*lower row*). Twenty hours after transfection, cells were incubated with 100 μg/ml cycloheximide for 4 h to allow efficient exit from the ER and fixed, permeabilized, and immunostained with an antibody to CD63. GFP-MCOLN1 is in *green*, and CD63 is in *red*; *yellow* indicates co-localization. *Scale bar,* 10 μm. *B,* cells expressing GFP-MCOLN1-WT or GFP-MCOLN1-RLK were harvested and subjected to Western blotting with an antibody to GFP. Note that both proteins are similarly expressed and can undergo cleavage and oligomerization. *C,* cells were transiently transfected with GFP-MCOLN1-WT, fixed, permeabilized, immunostained with anti-CD63 (*red*) and anti-Hrs-1 (*blue*), and analyzed by confocal fluorescence microscopy. The *arrow* points to a GFP-MCOLN1 expressing cell. Note that expression of MCOLN1 causes the aggregation of vesicular structures containing both CD63 and Hrs-1 in the perinuclear area. *White* indicates triple co-localization. *Scale bar,* 10 μm. *D,* quantification of the co-localization between vesicles containing GFP-MCOLN1-WT (*white bars*) or GFP-MCOLN1-^{44}RLK/AAA (RLK) (*black bars*) with CD63 and triple co-localization with Hrs-1 and CD63. The third set indicates co-localization of CD63 vesicles with Hrs-1 in cells expressing GFP-MCOLN1-WT or RLK. Results are mean ± S.D., $n = 30$ cells.

the binding. It is worth mentioning that although other members of the mucolipin family contain similar domains (^{37}KEECLREDLKFYM^{49} in MCOLN2 and ^{30}EELLLEDQMRRKLKFFF^{46} in MCOLN3), they are not capable of binding ALG-2 (data not shown).

Shibata *et al.* (55) classified ALG-2-binding proteins into two groups based on their ability to interact with an alternatively spliced ALG-2 isoform that lacks residues Gly^{121} and Phe^{122} (ALG-2$^{\Delta GF122}$). ABS-1 (ALG-2 binding sequence-1)-type proteins contain sequences that resemble the Alix P*X*Y repeat motif and lack the ability to bind to ALG-2$^{\Delta GF122}$, whereas ABS-2-type proteins interact with both ALG-2 and ALG-2$^{\Delta GF122}$. Recently, the crystal structure of the Ca^{2+}-free and Ca^{2+}-bound forms of ALG-2 have been solved revealing that binding of Ca^{2+} to the EF3 domain of ALG-2 causes a conformational change that makes a hydrophobic pocket accessible to the binding to the Alix P*X*Y motif (18). Deletion of Gly^{121} and Phe^{122} shortens a critical loop connecting ALG-2 α-helices 5 and 6, preventing the opening of the hydrophobic pocket after Ca^{2+} binding and thus explains the inability of ALG-2$^{\Delta GF122}$ to interact with Alix and other P*X*Y-containing proteins. We have found that MCOLN1 cannot interact with the ALG-2$^{\Delta GF122}$ isoform, indicating that it belongs to the ABS-1-type proteins. However, MCOLN1 differs from other ABS-1 proteins in that the MCOLN1 PRR region does not seem to be required for binding to ALG-2. Further experiments will be necessary to establish whether the charged hydrophobic sequence that constitutes the ALG-2-binding domain in MCOLN1 binds to the same hydrophobic pocket as the Alix P*X*Y motif (67). In any case, the identification of a new ALG-2-binding domain strengthens the idea that ALG-2 has structural flexibility of binding motifs (68) as happens in the case of calmodulin, which interacts with a large num-

ber of proteins to regulate their biological functions in response to Ca^{2+} stimuli (69).

While searching for Ca^{2+}-dependent binding partners of MCOLN1, we also identified the two members of the COPII coat cage Sec31A and Sec13. MCOLN1 interaction with both coat proteins was indirect, as depletion of ALG-2 by RNAi abolished the presence of Sec31A and Sec13 in MCOLN1 pull-downs. Recently, Okumura *et al.* (70) have showed that ALG-2 functions as a Ca^{2+} adaptor bridging Alix and TSG101, raising the question of whether ALG-2 might also link MCOLN1 and Sec31A at ER exit sites. We do not have any evidence to support this possibility. For example, the MCOLN1-RLK mutant exits the ER normally despite its inability to interact with ALG-2. Moreover, we did not observe differences in the distribution of endogenous Sec31A or in the trafficking of vesicular stomatitis virus G between ER and Golgi when comparing control and MLIV fibroblasts (data not shown), indicating that the absence of MCOLN1 does not affect COPII function. Finally, the trafficking defects described in MLIV occur at the endolysosomal pathway (15, 21, 22, 24–26, 34, 71–74), suggesting that MCOLN1 functions in this pathway rather than in ER-Golgi trafficking.

Release of luminal Ca^{2+} from organelles is known to play a crucial role in the regulation of many intracellular fusion/fission events, including homotypic fusion of endosomes (75, 76), heterotypic fusion of late endosomes with lysosomes (77), and reformation of lysosomes from hybrid compartments (77). Recent evidence showing that MCOLN1-*V432P* is an inwardly rectifying Ca^{2+}-selective channel (35, 36) supports the idea that MCOLN1 regulates transport of membrane components in the endosomal pathway. Moreover, we found that overexpression of MCOLN1 induces accumulation of enlarged aberrant endosomes that contain both early and late endosomal markers suggesting that MCOLN1 might mediate fusion/fission events. Interestingly, the accumulation of aberrant endosomes was greatly reduced upon overexpression of an MCOLN1 mutant incapable of interacting with ALG-2. There are several ways in which ALG-2 might regulate MCOLN1 function. First, ALG-2 might regulate MCOLN1 trafficking, explaining the decreased co-localization of MCOLN1-RLK with CD63. Consistent with this idea is the fact that calmodulin, also an EF-hand protein, interacts with a stretch of charged and hydrophobic residues located at the cytosolic tail of epidermal growth factor receptor (78), thus regulating epidermal growth factor receptor trafficking and signaling (79). Second, binding of ALG-2 might induce a conformational change in MCOLN1 that alters its channel activity. In agreement with this possibility, several reports indicate that variations in cytosolic Ca^{2+} concentration may modulate the permeability of the MCOLN1 channel (34, 80). Finally, we favor a third possibility in which ALG-2 acts as a Ca^{2+}-dependent adaptor bringing together proteins implicated in endosomal biogenesis. The fact that ALG-2 forms homodimers and each monomer has one peptide-binding site (68) suggests that ALG-2 may bridge two interacting proteins, as has been described for Alix and TSG101 (70). Release of luminal Ca^{2+} mediated by MCOLN1 could then promote interaction with ALG-2 along with the ALG-2-dependent recruitment of other proteins implicated in fusion/fission events.

Overall, our data provide new insight into the molecular basis for the regulation of MCOLN1 function by Ca^{2+} and suggest a novel role for ALG-2 as a Ca^{2+} sensor at endosomes/lysosomes.

Acknowledgments—We thank the members of the NHLBI Proteomics Core Facility for assistance. We also appreciate the editorial advice of the National Institutes of Health Fellows Editorial Board.

REFERENCES

1. Bach, G. (2001) *Mol. Genet. Metab.* **73,** 197–203
2. Amir, N., Zlotogora, J., and Bach, G. (1987) *Pediatrics* **79,** 953–959
3. Altarescu, G., Sun, M., Moore, D. F., Smith, J. A., Wiggs, E. A., Solomon, B. I., Patronas, N. J., Frei, K. P., Gupta, S., Kaneski, C. R., Quarrell, O. W., Slaugenhaupt, S. A., Goldin, E., and Schiffmann, R. (2002) *Neurology* **59,** 306–313
4. Bach, G., Cohen, M. M., and Kohn, G. (1975) *Biochem. Biophys. Res. Commun.* **66,** 1483–1490
5. Tellez-Nagel, I., Rapin, I., Iwamoto, T., Johnson, A. B., Norton, W. T., and Nitowsky, H. (1976) *Arch. Neurol.* **33,** 828–835
6. Bach, G., Ziegler, M., Kohn, G., and Cohen, M. M. (1977) *Am. J. Hum. Genet.* **29,** 610–618
7. Crandall, B. F., Philippart, M., Brown, W. J., and Bluestone, D. A. (1982) *Am. J. Med. Genet.* **12,** 301–308
8. Folkerth, R. D., Alroy, J., Lomakina, I., Skutelsky, E., Raghavan, S. S., and Kolodny, E. H. (1995) *J. Neuropathol. Exp. Neurol.* **54,** 154–164
9. Chen, C. S., Bach, G., and Pagano, R. E. (1998) *Proc. Natl. Acad. Sci. U.S.A.* **95,** 6373–6378
10. Slaugenhaupt, S. A., Acierno, J. S., Jr., Helbling, L. A., Bove, C., Goldin, E., Bach, G., Schiffmann, R., and Gusella, J. F. (1999) *Am. J. Hum. Genet.* **65,** 773–778
11. Bargal, R., Avidan, N., Ben-Asher, E., Olender, Z., Zeigler, M., Frumkin, A., Raas-Rothschild, A., Glusman, G., Lancet, D., and Bach, G. (2000) *Nat. Genet.* **26,** 118–123
12. Bassi, M. T., Manzoni, M., Monti, E., Pizzo, M. T., Ballabio, A., and Borsani, G. (2000) *Am. J. Hum. Genet.* **67,** 1110–1120
13. Sun, M., Goldin, E., Stahl, S., Falardeau, J. L., Kennedy, J. C., Acierno, J. S., Jr., Bove, C., Kaneski, C. R., Nagle, J., Bromley, M. C., Colman, M., Schiffmann, R., and Slaugenhaupt, S. A. (2000) *Hum. Mol. Genet.* **9,** 2471–2478
14. Puertollano, R., and Kiselyov, K. (2009) *Am. J. Physiol. Renal Physiol.* **296,** F1245–F1254
15. Pryor, P. R., Reimann, F., Gribble, F. M., and Luzio, J. P. (2006) *Traffic* **7,** 1388–1398
16. Vergarajauregui, S., and Puertollano, R. (2006) *Traffic* **7,** 337–353
17. Vergarajauregui, S., Oberdick, R., Kiselyov, K., and Puertollano, R. (2008) *Biochem. J.* **410,** 417–425
18. Kiselyov, K., Chen, J., Rbaibi, Y., Oberdick, D., Tjon-Kon-Sang, S., Shcheynikov, N., Muallem, S., and Soyombo, A. (2005) *J. Biol. Chem.* **280,** 43218–43223
19. LaPlante, J. M., Ye, C. P., Quinn, S. J., Goldin, E., Brown, E. M., Slaugenhaupt, S. A., and Vassilev, P. M. (2004) *Biochem. Biophys. Res. Commun.* **322,** 1384–1391
20. Cantiello, H. F., Montalbetti, N., Goldmann, W. H., Raychowdhury, M. K., Gonzalez-Perrett, S., Timpanaro, G. A., and Chasan, B. (2005) *Pfluegers Arch.* **451,** 304–312
21. Soyombo, A. A., Tjon-Kon-Sang, S., Rbaibi, Y., Bashllari, E., Bisceglia, J., Muallem, S., and Kiselyov, K. (2006) *J. Biol. Chem.* **281,** 7294–7301
22. Dong, X. P., Cheng, X., Mills, E., Delling, M., Wang, F., Kurz, T., and Xu, H. (2008) *Nature* **455,** 992–996
23. Piper, R. C., and Luzio, J. P. (2004) *Trends Cell Biol.* **14,** 471–473
24. Treusch, S., Knuth, S., Slaugenhaupt, S. A., Goldin, E., Grant, B. D., and Fares, H. (2004) *Proc. Natl. Acad. Sci. U.S.A.* **101,** 4483–4488
25. LaPlante, J. M., Sun, M., Falardeau, J., Dai, D., Brown, E. M., Slaugenhaupt, S. A., and Vassilev, P. M. (2006) *Mol. Genet. Metab.* **89,** 339–348
26. Vergarajauregui, S., Connelly, P. S., Daniels, M. P., and Puertollano, R.

(2008) *Hum. Mol. Genet.* **17,** 2723–2737
27. Venkatachalam, K., Long, A. A., Elsaesser, R., Nikolaeva, D., Broadie, K., and Montell, C. (2008) *Cell* **135,** 838–851
28. Vergarajauregui, S., and Puertollano, R. (2008) *Autophagy* **4,** 832–834
29. Miedel, M. T., Rbaibi, Y., Guerriero, C. J., Colletti, G., Weixel, K. M., Weisz, O. A., and Kiselyov, K. (2008) *J. Exp. Med.* **205,** 1477–1490
30. Venugopal, B., Mesires, N. T., Kennedy, J. C., Curcio-Morelli, C., Laplante, J. M., Dice, J. F., and Slaugenhaupt, S. A. (2009) *J. Cell. Physiol.* **219,** 344–353
31. Luzio, J. P., Bright, N. A., and Pryor, P. R. (2007) *Biochem. Soc. Trans.* **35,** 1088–1091
32. Rodríguez, A., Webster, P., Ortego, J., and Andrews, N. W. (1997) *J. Cell Biol.* **137,** 93–104
33. Gordon, P. B., Holen, I., Fosse, M., Røtnes, J. S., and Seglen, P. O. (1993) *J. Biol. Chem.* **268,** 26107–26112
34. LaPlante, J. M., Falardeau, J., Sun, M., Kanazirska, M., Brown, E. M., Slaugenhaupt, S. A., and Vassilev, P. M. (2002) *FEBS Lett.* **532,** 183–187
35. Xu, H., Delling, M., Li, L., Dong, X., and Clapham, D. E. (2007) *Proc. Natl. Acad. Sci. U.S.A.* **104,** 18321–18326
36. Grimm, C., Cuajungco, M. P., van Aken, A. F., Schnee, M., Jörs, S., Kros, C. J., Ricci, A. J., and Heller, S. (2007) *Proc. Natl. Acad. Sci. U.S.A.* **104,** 19583–19588
37. Lo, K. W., Zhang, Q., Li, M., and Zhang, M. (1999) *Biochemistry* **38,** 7498–7508
38. Maki, M., Kitaura, Y., Satoh, H., Ohkouchi, S., and Shibata, H. (2002) *Biochim. Biophys. Acta* **1600,** 51–60
39. Tarabykina, S., Mollerup, J., Winding, P., and Berchtold, M. W. (2004) *Front. Biosci.* **9,** 1817–1832
40. Missotten, M., Nichols, A., Rieger, K., and Sadoul, R. (1999) *Cell Death Differ.* **6,** 124–129
41. Vito, P., Pellegrini, L., Guiet, C., and D'Adamio, L. (1999) *J. Biol. Chem.* **274,** 1533–1540
42. Katoh, K., Suzuki, H., Terasawa, Y., Mizuno, T., Yasuda, J., Shibata, H., and Maki, M. (2005) *Biochem. J.* **391,** 677–685
43. Yamasaki, A., Tani, K., Yamamoto, A., Kitamura, N., and Komada, M. (2006) *Mol. Biol. Cell* **17,** 4876–4887
44. la Cour, J. M., Mollerup, J., and Berchtold, M. W. (2007) *Biochem. Biophys. Res. Commun.* **353,** 1063–1067
45. Shibata, H., Suzuki, H., Yoshida, H., and Maki, M. (2007) *Biochem. Biophys. Res. Commun.* **353,** 756–763
46. Mahul-Mellier, A. L., Hemming, F. J., Blot, B., Fraboulet, S., and Sadoul, R. (2006) *J. Neurosci.* **26,** 542–549
47. Rao, R. V., Poksay, K. S., Castro-Obregon, S., Schilling, B., Row, R. H., del Rio, G., Gibson, B. W., Ellerby, H. M., and Bredesen, D. E. (2004) *J. Biol. Chem.* **279,** 177–187
48. la Cour, J. M., Mollerup, J., Winding, P., Tarabykina, S., Sehested, M., and Berchtold, M. W. (2003) *Am. J. Pathol.* **163,** 81–89
49. Wang, G., Wu, W. W., Zeng, W., Chou, C. L., and Shen, R. F. (2006) *J. Proteome Res.* **5,** 1214–1223
50. Hoffert, J. D., Wang, G., Pisitkun, T., Shen, R. F., and Knepper, M. A. (2007) *J. Proteome Res.* **6,** 3501–3508
51. Fath, S., Mancias, J. D., Bi, X., and Goldberg, J. (2007) *Cell* **129,** 1325–1336
52. Satoh, H., Shibata, H., Nakano, Y., Kitaura, Y., and Maki, M. (2002) *Biochem. Biophys. Res. Commun.* **291,** 1166–1172
53. Satoh, H., Nakano, Y., Shibata, H., and Maki, M. (2002) *Biochim. Biophys. Acta* **1600,** 61–67
54. Tarabykina, S., Møller, A. L., Durussel, I., Cox, J., and Berchtold, M. W. (2000) *J. Biol. Chem.* **275,** 10514–10518
55. Shibata, H., Suzuki, H., Kakiuchi, T., Inuzuka, T., Yoshida, H., Mizuno, T., and Maki, M. (2008) *J. Biol. Chem.* **283,** 9623–9632
56. Shibata, H., Yamada, K., Mizuno, T., Yorikawa, C., Takahashi, H., Satoh, H., Kitaura, Y., and Maki, M. (2004) *J. Biochem.* **135,** 117–128
57. Trioulier, Y., Torch, S., Blot, B., Cristina, N., Chatellard-Causse, C., Verna, J. M., and Sadoul, R. (2004) *J. Biol. Chem.* **279,** 2046–2052
58. Chen, C., and Sytkowski, A. J. (2005) *Biochem. Biophys. Res. Commun.* **333,** 51–57
59. Hwang, I. S., Jung, Y. S., and Kim, E. (2002) *FEBS Lett.* **529,** 183–187
60. Babst, M., Wendland, B., Estepa, E. J., and Emr, S. D. (1998) *EMBO J.* **17,** 2982–2993
61. Fujita, H., Yamanaka, M., Imamura, K., Tanaka, Y., Nara, A., Yoshimori, T., Yokota, S., and Himeno, M. (2003) *J. Cell Sci.* **116,** 401–414
62. Dunn, K. C., Aotaki-Keen, A. E., Putkey, F. R., and Hjelmeland, L. M. (1996) *Exp. Eye Res.* **62,** 155–169
63. Aukunuru, J. V., Sunkara, G., Bandi, N., Thoreson, W. B., and Kompella, U. B. (2001) *Pharm. Res.* **18,** 565–572
64. Miedel, M. T., Weixel, K. M., Bruns, J. R., Traub, L. M., and Weisz, O. A. (2006) *J. Biol. Chem.* **281,** 12751–12759
65. Christensen, K. A., Myers, J. T., and Swanson, J. A. (2002) *J. Cell Sci.* **115,** 599–607
66. Draeby, I., Woods, Y. L., la Cour, J. M., Mollerup, J., Bourdon, J. C., and Berchtold, M. W. (2007) *Arch. Biochem. Biophys.* **467,** 87–94
67. Suzuki, H., Kawasaki, M., Inuzuka, T., Okumura, M., Kakiuchi, T., Shibata, H., Wakatsuki, S., and Maki, M. (2008) *Structure* **16,** 1562–1573
68. Suzuki, H., Kawasaki, M., Inuzuka, T., Okumura, M., Kakiuchi, T., Shibata, H., Wakatsuki, S., and Maki, M. (2009) *Biochem. Soc. Trans.* **37,** 190–194
69. Yap, K. L., Kim, J., Truong, K., Sherman, M., Yuan, T., and Ikura, M. (2000) *J. Struct. Funct. Genomics* **1,** 8–14
70. Okumura, M., Ichioka, F., Kobayashi, R., Suzuki, H., Yoshida, H., Shibata, H., and Maki, M. (2009) *Biochem. Biophys. Res. Commun.* **386,** 237–241
71. Bach, G. (2005) *Pflugers Arch* **451,** 313–317
72. Fares, H., and Greenwald, I. (2001) *Nat. Genet.* **28,** 64–68
73. Manzoni, M., Monti, E., Bresciani, R., Bozzato, A., Barlati, S., Bassi, M. T., and Borsani, G. (2004) *FEBS Lett.* **567,** 219–224
74. Thompson, E. G., Schaheen, L., Dang, H., and Fares, H. (2007) *BMC Cell Biol.* **8,** 54
75. Holroyd, C., Kistner, U., Annaert, W., and Jahn, R. (1999) *Mol. Biol. Cell* **10,** 3035–3044
76. Yan, Q., Sun, W., McNew, J. A., Vida, T. A., and Bean, A. J. (2004) *J. Biol. Chem.* **279,** 18270–18276
77. Pryor, P. R., Mullock, B. M., Bright, N. A., Gray, S. R., and Luzio, J. P. (2000) *J. Cell Biol.* **149,** 1053–1062
78. Martín-Nieto, J., and Villalobo, A. (1998) *Biochemistry* **37,** 227–236
79. Tebar, F., Villalonga, P., Sorkina, T., Agell, N., Sorkin, A., and Enrich, C. (2002) *Mol. Biol. Cell* **13,** 2057–2068
80. Raychowdhury, M. K., González-Perrett, S., Montalbetti, N., Timpanaro, G. A., Chasan, B., Goldmann, W. H., Stahl, S., Cooney, A., Goldin, E., and Cantiello, H. F. (2004) *Hum. Mol. Genet.* **13,** 617–627